Progress in Scale Modeling, an International Journal

Volume 2
Issue 2 *Special issue of Scale Modeling for Fire Research*
Article 7

2021

Open-field scale-model experiments of fire whirls over L-shaped line fires

Yuto Iga
Yamagata University

Kazunori Kuwana
Yamagata University, kuwana@rs.tus.ac.jp

Kozo Sekimoto
University of Kentucky, skozo@ac.auone-net.jp

Yuji Nakamura
Toyohashi University of Technology, yuji@me.tut.ac.jp

Recommended Citation
Iga, Yuto; Kuwana, Kazunori; Sekimoto, Kozo; and Nakamura, Yuji (2021) "Open-field scale-model experiments of fire whirls over L-shaped line fires," *Progress in Scale Modeling, an International Journal*: Vol. 2 : Iss. 2 , Article 7.
DOI: https://doi.org/10.13023/psmij.2021.02-02-07
Available at: https://uknowledge.uky.edu/psmij/vol2/iss2/7

Open-field scale-model experiments of fire whirls over L-shaped line fires

Category

Rapid Communication

Abstract

This paper presents the results of open-field scale-model experiments of fire-whirl formation over line fires. L-shaped line fires were burned in crosswinds, and the processes of fire-whirl formation were observed. The flame height was measured using an image-processing technique, while two-dimensional velocity components were measured at two different locations using ultrasonic anemometers. Two tests were selected for comparison: test A, in which intense fire whirls repeatedly formed, and test B, in which no whirls were observed. In test A, the wind flow was bent by the fire plume, creating swirling flows near the burning area, thereby forming fire whirls. On the other hand, the crosswind in test B was too fast to be affected by the fire plume. These results confirmed the existence of critical wind velocity to form intense fire whirls. The critical wind velocity, approximately 1 m/s, agreed with the scaling law on the critical wind velocity which was previously developed based on similar experiments of a smaller scale.

Keywords

Fire whirl, Line fire; Crosswind, Critical wind velocity, Scaling analysis

Progress in Scale Modeling, an International Journal, Vol. 2, Issue 2 (2021) Article 02-02-07, pp. 1–7
https://doi.org/10.13023/psmij.2021.02-02-07

Open-field scale-model experiments of fire whirls over L-shaped line fires

Yuto Iga [a], Kazunori Kuwana [a,*], Kozo Sekimoto [b], Yuji Nakamura [c]

[a] *Department of Chemistry and Chemical Engineering, Yamagata University, 4-3-16 Jonan, Yonezawa, Yamagata 992-8510, Japan*

[b] *Institute of Research for Technology Development (IR4TD), University of Kentucky, Lexington, KY 40506-0503, USA*

[c] *Department of Mechanical Engineering, Toyohashi University of Technology, 1-1 Hibarigaoka, Tempaku, Toyohashi, Aichi 441-8580, Japan*

E-mail: kuwana@yz.yamagata-u.ac.jp

Received January 13, 2021, Accepted January 19, 2021

Abstract

This paper presents the results of open-field scale-model experiments of fire-whirl formation over line fires. L-shaped line fires were burned in crosswinds, and the processes of fire-whirl formation were observed. The flame height was measured using an image-processing technique, while two-dimensional velocity components were measured at two different locations using ultrasonic anemometers. Two tests were selected for comparison: test A, in which intense fire whirls repeatedly formed, and test B, in which no whirls were observed. In test A, the wind flow was bent by the fire plume, creating swirling flows near the burning area, thereby forming fire whirls. On the other hand, the crosswind in test B was too fast to be affected by the fire plume. These results confirmed the existence of critical wind velocity to form intense fire whirls. The critical wind velocity, approximately 1 m/s, agreed with the scaling law on the critical wind velocity which was previously developed based on similar experiments of a smaller scale.

Keywords: Fire whirl; Line fire; Crosswind; Critical wind velocity; Scaling analysis

Introduction

Fire whirls have caused severe damages in urban and wildland fires [1–3]. It is understood that fire whirls form because of the interaction between fires and crosswinds [2, 3]. Refs. [2] and [3] are pioneering studies that reported the results of scale-model experiments of fire whirls formed in crosswinds. These experiments were designed based on scaling considerations (see Ref. [4] for discussion of scaling laws).

The use of a wind tunnel enables careful control of crosswind velocity [2–13]. It is now established that there is a narrow range of crosswind velocity (the critical wind velocity) that leads to the formation of intense fire whirls. On the other hand, finding critical conditions in outdoor experiments is challenging. Soma and Saito [3] conducted a large-scale outdoor experiment, which consisted of a burning area of approximately 400 m^2. They successfully observed the formation of fire whirls when the crosswind velocity was 1–1.5 m/s, whereas, in another test, the crosswind velocity was too high (4–5 m/s) to form fire whirls. Because the number of successful tests is limited, it is still unclear how and when fire whirls form in open fields. Such insights will enable accurate prediction of fire-whirl formation in actual urban and wildland fires, an essential step toward developing effective firefighting strategies.

This paper reports our efforts to understand further the critical condition of fire-whirl formation in an open field. A series of open-field scale-model experiments were conducted, in which fire whirls formed over L-shaped line fires. The time histories of flame height evolution were obtained by image processing, and two-dimensional velocity vectors were measured at two different locations using ultrasonic anemometers. Two

Progress in Scale Modeling
AN INTERNATIONAL JOURNAL
https://uknowledge.uky.edu/psmij/

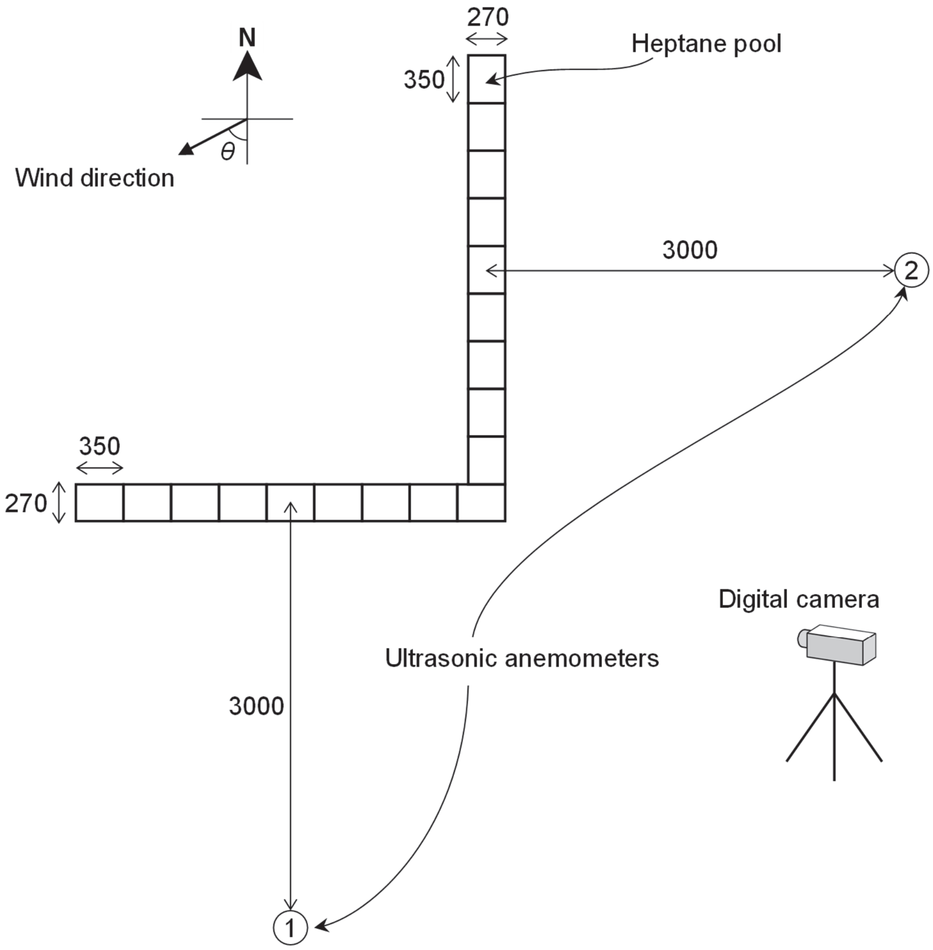

Fig. 1. Experimental setup (unit, mm).

(a) Original image

(b) Binary image

Fig. 2. Image processing to obtain flame-height evolution.

conditions were selected: a condition in which stable and intense fire whirls formed and another condition in which no whirls were observed. Differences in flow patterns between the two tests are discussed.

Experimental method

Fig. 1 shows the L-shaped burning area of the present experiment. The burning area consists of 18 rectangular-shaped open-top pans (27-cm wide × 35-cm long) buried in a surrounding sand layer such that their top rims were flush with the sand surface. The bottom half of each pan was filled with water, on top of which n-heptane was filled to the rim. Ignition was made by a burner, and all 18 pool fires were ignited in less than 5 s. An ultrasonic anemometer (Gill WindSonic; accuracy, ±2% or ±0.01 m/s) was placed 3 m away from each side to record the time history of two-dimensional velocity vectors at 10 Hz. The anemometer placed to the south of the burning area is referred to as anemometer 1, whereas the one placed to the east as anemometer 2 (see Fig. 1). The vertical location from the ground of the

(a) Original image (b) Binary image

Fig. 3. A typical fire whirl formed in test A.

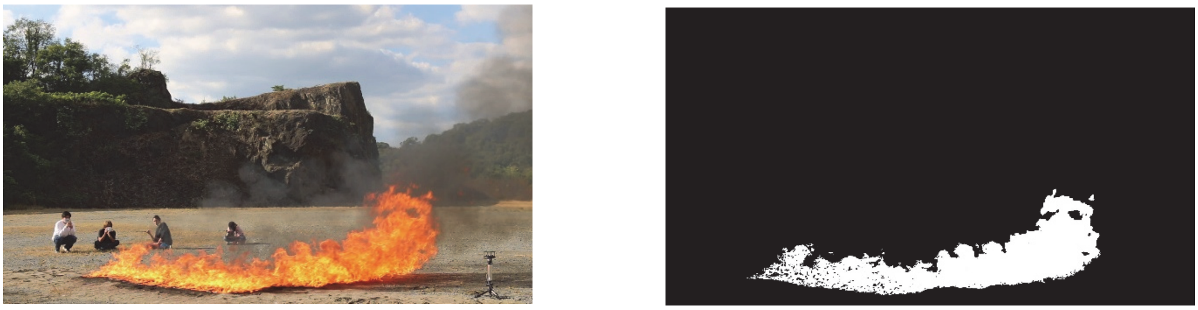

(a) Original image (b) Binary image

Fig. 4. Burning area in test B.

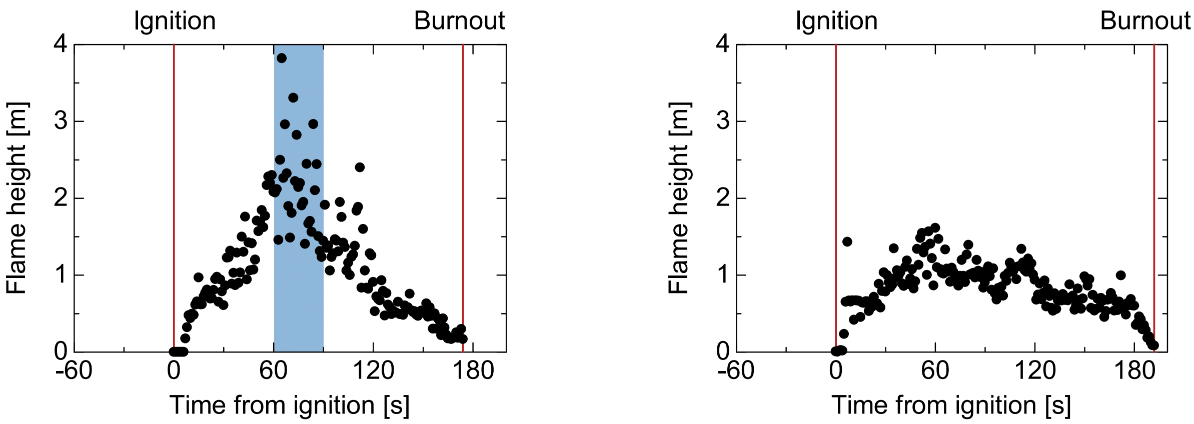

(a) Test A (b) Test B

Fig. 5. Flame-height evolution in tests A and B. The shaded region in (a) shows the period (between 60 and 90 s) in which intense fire whirls formed.

anemometers was 0.5 m. A preliminary test confirmed that the crosswind velocity at 1.5 m showed little difference from that at 0.5 m; therefore, the data at 0.5 m was assumed to represent the crosswind velocity at that location.

A digital camera (SONY HDR-CX560V, 60 Hz) was used to record the flame shape, from which the evolution of the instantaneous flame height was obtained. Fig. 2a shows a typical image, and it was converted to the binary image shown in Fig. 2b. Here, the flame region is defined as a set of pixels whose red component is between 200 and 255, and the blue component is less than or equal to 100.

Results and discussion

Two tests, called tests A and B, are selected to discuss the formation mechanism of fire whirls. In test A, stable and intense fire whirls formed as shown in Fig. 3. On the other hand, in test B, the flame was tilted downstream, and no fire whirls were observed as shown in Fig. 4.

Fig. 5 shows flame-height evolution in tests A and B. In test A, intense fire whirls formed, leading to in-

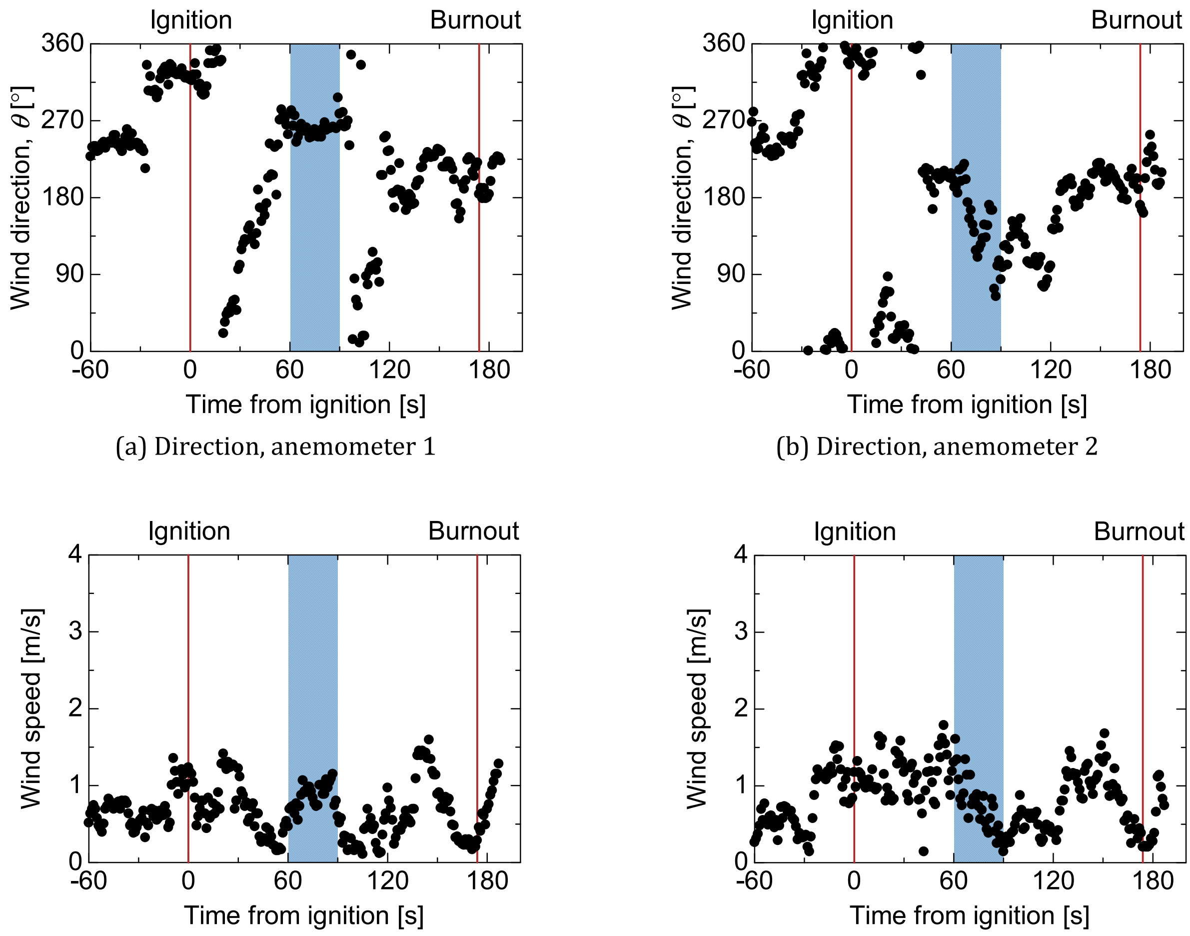

(a) Direction, anemometer 1 (b) Direction, anemometer 2

(c) Speed, anemometer 1 (d) Speed, anemometer 2

Fig. 6. Wind direction and speed measured in test A. The shaded region shows the period (between 60 and 90 s) in which intense fire whirls formed.

creased flame heights. Especially in the period between 60 and 90 s after ignition, stable fire whirls were observed, and the flame height constantly exceeded 2 m. In contrast, the flame height was less than 1.5 m in most of test B. Fig. 6 shows the direction and speed of wind measured in test A, and angle θ, defined in Fig. 1, is used to show the wind direction. Before ignition, wind directions and speeds measured by the two anemometers were similar, and a north wind ($\theta \approx 0$ or 360°) of approximately 1 m/s was recorded at the time of ignition. After ignition, the presence of the burning area significantly changed the wind speed and direction. When the wind direction at anemometer 2 was from north to south, the wind speed at anemometer 1 was lower than that at anemometer 2 because the plume of the burning area blocked the wind, supporting Williams [14] who discussed that a burning area could change the topography as the obstacle that interacts with the wind.

Intense fire whirls were formed at ~60 s after ignition when the anemometer 1 recorded wind blowing from west to east with slightly less than 1 m/s. Throughout the period from 60 to 90 s, when intense

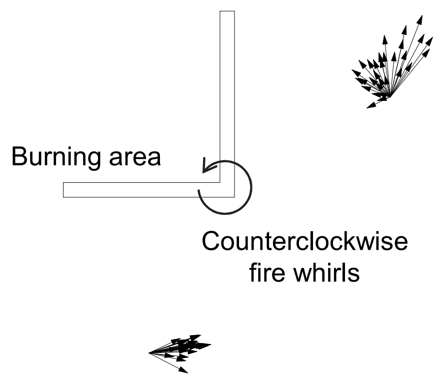

Fig. 7. Wind vectors from 60 to 90 s in test A.

fire whirls repeatedly formed, the wind direction at anemometer 1 was steadily from west to east at a speed close to 1 m/s. The wind direction at anemometer 2 (on the downstream side of the west wind) was 90° < θ < 180°, indicating an entrainment wind toward the fire plume. Fig. 7 depicts wind vectors during this period. Fire whirls rotating in counterclockwise directions

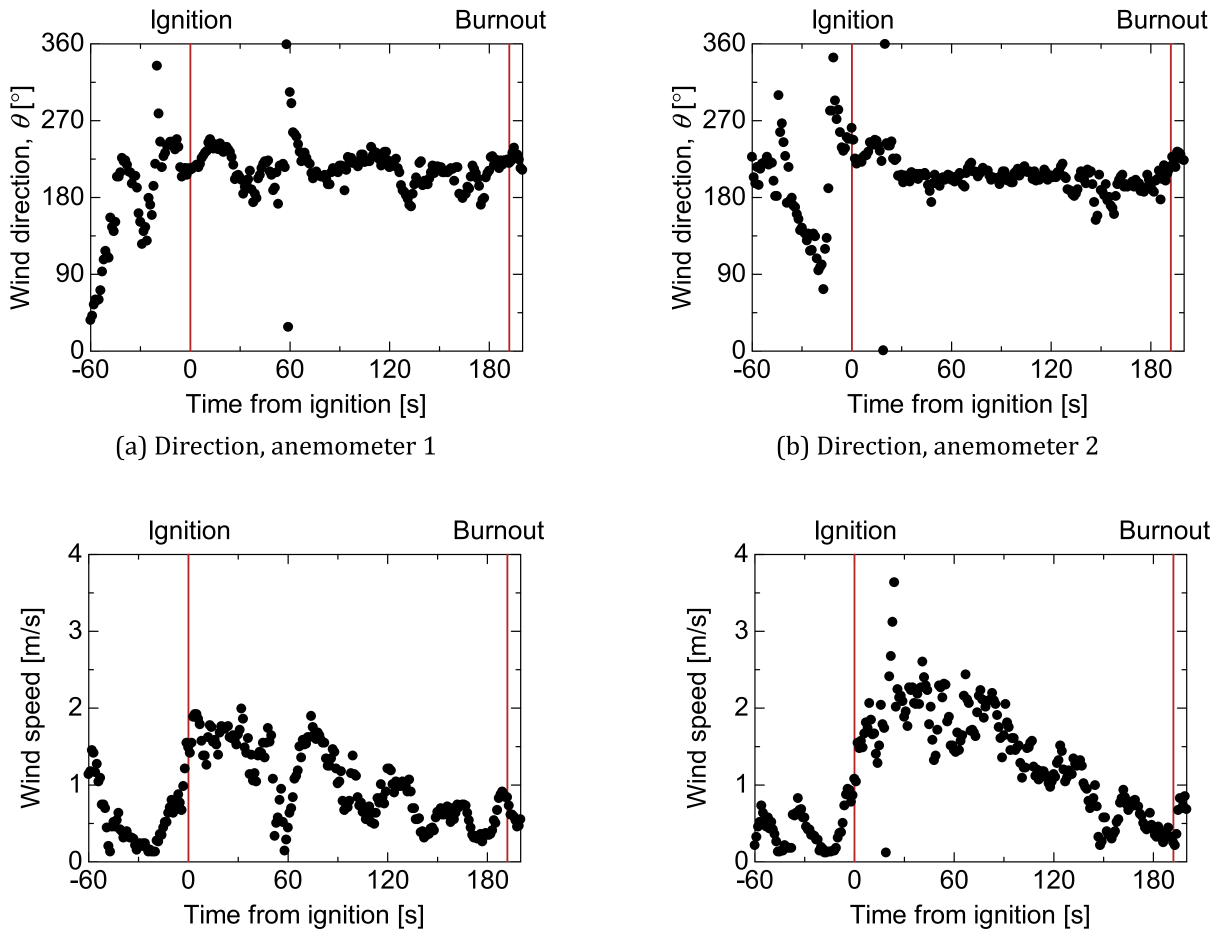

(a) Direction, anemometer 1 (b) Direction, anemometer 2

(c) Speed, anemometer 1 (d) Speed, anemometer 2

Fig. 8. Wind direction and speed measured in test B.

formed near the corner of the burning area as evidenced in Fig. 3. The fire plume changed the wind direction, creating a swirling flow that led to the formation of fire whirls. The critical wind velocity in the present experiment was found to be approximately 1 m/s.

Fig. 8 shows the direction and speed of wind measured in test B. The wind directions from −60 to −30 s were somewhat different between anemometers 1 and 2. However, they were similar at both the anemometers from −30 s to the time of ignition. After ignition, the wind direction was not affected by the fire plume and therefore it did not change significantly, because the wind speed was higher than that in test A. Anemometer 2 recorded the wind speed exceeding 1.5 m/s until ~100 s. Fig. 9 depicts wind vectors between 60 and 90 s in test B. Contrarily to Fig. 7, the wind speed was too high to be significantly affected by the fire plume. Although the wind speed slowed after 100 s, some of the fuel pans nearly burned out at that time, and it was impossible to form intense fire whirls. Comparing tests A and B indicates that both the wind direction and speed need to be in specific ranges to form intense fire whirls.

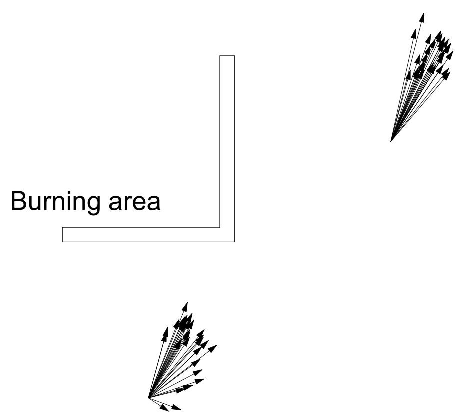

Fig. 9. Wind vectors from 60 to 90 s in test B.

Finally, scaling laws that describe the critical condition to form fire whirls are discussed. Here, the configuration of the burning area can be regarded as a curved line fire, and our experimental observations indicate that fire whirls tend to form over line fires, especially near regions of large curvatures.

Refs. [5] and [6] proposed a scaling law that the

Table 1. The values of the critical Froude numbers.

	H [m]	U_c [m/s]	$U_c/(gH)^{1/2}$ [–]
Ref. [9]	0.1	0.2–0.3	0.20–0.30
This study	1	1	0.32

critical wind velocity, U_c, is of the same order as the buoyant velocity, U_b, of the fire plume. As U_b can be estimated using the flame height, H, as $U_b \sim (gH)^{1/2}$, where g is the acceleration of gravity, the following expression for U_c or the critical Froude number $U_c/(gH)^{1/2}$ is obtained:

$$U_c \sim (gH)^{1/2} \text{ or } U_c/(gH)^{1/2} = \text{constant} \quad (1)$$

The flame height, H, in Eq. (1) is the value without the formation of fire whirls, which is approximately 1 m according to the data shown in Fig. 5. Ref. [9] reported $U_c =$ 0.2–0.3 m/s in a laboratory-scale, wind-tunnel experiment. Although Ref. [9] did not report the value of H, it is estimated to be approximately 0.1 m, based on the flame-height data of a similar experiment presented in Ref. [15]. As shown in Table 1, the values of the critical Froude number are similar between the experiments of two different scales, verifying the scaling law in the open-field experiment.

The flame height, H, of an infinitely-long line fire is given by the line width, w, and the heat release rate per unit length, $\dot{Q}'$ [W/m]. In a dimensionless form,

$$\frac{H}{w} = f\left(\frac{\dot{Q}'}{\rho_0 c_0 T_0 g^{1/2} w^{3/2}}\right) \quad (2)$$

Here, f denotes a certain function, and ρ_0, c_0, and T_0 are respectively the density, the specific heat, and the temperature of the ambient air. In the limit of thin line fires, i.e., $w/H \to 0$, the flame height does not depend on w, leading to the following scaling law:

$$\frac{H}{w} \sim \left(\frac{\dot{Q}'}{\rho_0 c_0 T_0 g^{1/2} w^{3/2}}\right)^{2/3} \quad (3)$$

Combining (1) and (3), one obtains

$$U_c \sim \left(\frac{g\dot{Q}'}{\rho_0 c_0 T_0}\right)^{1/3} \quad (4)$$

Since g, ρ_0, c_0, and T_0 can be regarded as constant, Eq. (4) suggests that U_c be proportional to $\dot{Q}'^{1/3}$.

The value of $\dot{Q}'$ in this study was about 0.25 MW/m. On the other hand, Mueller et al. [16] conducted large-scale field experiments and estimated that the value of $\dot{Q}'$ was as much as 4.4 MW/m for surface fires, whereas that for crown fires (canopy fires) was as much as 21 MW/m. Eq. (4) then suggests that $U_c \approx 2.6$ m/s for the surface fires and 4.4 m/s for the crown fires. Further studies are necessary to validate the proposed scaling law, Eq. (4).

Conclusions

Open-field scale-model experiments were conducted to understand the formation mechanisms of fire whirls over line fires. It was found that when the wind crossed the fire area, it was twisted near the fire area and formed a fire whirl. When the crosswind velocity was faster than ~1.5 m/s, the inertial force of wind dominated the buoyancy force created by the burning area, and no whirls formed, indicating the existence of the critical wind velocity to form intense fire whirls. A previously proposed scaling law [5, 6] for the critical condition was validated by comparing the present results with literature data of a different scale. Scaling analysis suggests that the critical wind velocity, U_c, should increase as $U_c \sim \dot{Q}'^{1/3}$, where $\dot{Q}'$ is the heat release rate per unit length.

Acknowledgments

This work was supported in part by Kajima Foundation and JSPS KAKENHI Grant Numbers 19H01807 and 19K22023.

References

[1] Graham, H. E., “Fire whirlwinds,” Bull. Am. Meteorol. Soc. 36: 99–103, 1955.

[2] Emori, R. I., Saito, K., “Model experiment of hazardous forest fire whirl,” Fire Technol. 18: 319–327, 1982.

[3] Soma, S, Saito, K., “Reconstruction of fire whirls using scale models,” Combust. Flame 86: 269–284, 1991.

[4] Williams, F. A., “Scaling considerations for fire whirls,” Progress in Scale Modeling, an International Journal 1: Article 2, 1–4.

[5] Kuwana, K., Sekimoto, K., Saito, K., Williams, F. A., Hayashi, Y., Masuda, H., “Can we predict the occurrence of extreme fire whirls?” AIAA J. 45: 16–19, 2007.

[6] Kuwana, K., Sekimoto, K., Saito, K., Williams, F. A., “Scaling fire whirls,” Fire Saf. J. 43: 252–257, 2008.

[7] Kuwana, K., Sekimoto, K., Saito, K., “Wind-tunnel fire-whirl experiments using a scale model,” J. Chem. Eng. Jpn. 43: 952–955, 2010.

[8] Shinohara, M., Matsushima, S., “Formation of fire whirls: Experimental verification that a counter-rotating vortex pair is a possible origin of fire whirls,” Fire Saf. J. 54: 144–153, 2012.

[9] Kuwana, K., Sekimoto, K., Minami, T., Tashiro, T.,

Saito, K., "Scale-model experiments of moving fire whirl over a line fire," Proc. Combust. Inst. 34: 2625–2631, 2013.
[10] Zhou, K., Liu, N., Yuan, X., "Effect of wind on fire whirl over a line fire," Fire Technol. 52: 865–875, 2016.
[11] Himoto, K., Naruse, T., "Probabilistic aspect of fire whirl generation around an L-shaped fire source in a crosswind," Fire Saf. J. 88: 89–95, 2017.
[12] Sasaki, T., Igari, M., Kuwana, K., "Fire whirls behind an L-shaped wall in a crossflow," Combust. Flame 197: 197–203, 2018.
[13] Shinohara, M., "Effects of wind speed and heat release rate on the vortex strength and size of fire whirls without an inner core of flame," Fire Saf. J. (in press).
[14] Williams, F. A., "Urban and wildland fire phenomenology," Prog. Energy Combust. Sci. 8: 317–354, 1982.
[15] Iga, Y., Kuwana, K., "Generation of fire whirls over a line fire in a crossflow: an experimental study on the role of near-ground flow," 27th International Colloquium on the Dynamics of Explosions and Reactive Systems (ICDERS), Beijing, China, July 28–August 2, 2019.
[16] Mueller, E. V., Skowronski, N., Clark, K., Gallagher, M., Kremens, R., Thomas, J. C., Houssami, M. El, Filkov, A., Hadden, R. M., Mell, W., Simeoni, A., "Utilization of remote sensing techniques for the quantification of fire behavior in two pine stands," Fire Saf. J. 91: 845–854, 2017.